IPC

Indonesian Physics Communication

Department of Physics, Universitas Riau, Pekanbaru, Indonesia
p-ISSN 1412-2960 | e-ISSN 2579-521X

Vol. 21 | No. 3
November 2024

Web: https://kfi.ejournal.unri.ac.id
E-mail: kfi@ejournal.unri.ac.id

Areca-nut waste-derived carbon porous for sustainable electrode materials: A brief study for green-supercapacitor

Nursyafni Nursyafni[1], Julnaidi[2], Erman Taer[1,*]

[1]Department of Physics, Universitas Riau, Pekanbaru 28293, Indonesia
[2]Department of Mechanical Engineering, Pekanbaru College of Technology, Pekanbaru 28125, Indonesia

*Corresponding author: erman.taer@lecturer.unri.ac.id

ABSTRACT

Biomass-based porous carbon is an exceptional material with unique nano-morphological properties and a high surface area, making it an ideal candidate for improving the performance of supercapacitor electrodes. Herein, activated carbon derived novel areca-nut waste (ANW) as electrodes materials were successfully produced using a simple method. The process involved drying the ANW using pre-carbonization, chemical activation, and high-temperature pyrolysis. The zinc chloride was selected as chemical catalytic in 1 m/l solution. Subsequently, porous carbon was produced at different physical activation temperatures of 800°C, 850°C, and 900°C. The activated carbon was converted into coin-like design with an additional adhesive of PVA. The electrochemical properties were assessed using a two-electrode system in a 1 M H_2SO_4 electrolyte. The ANW-based supercapacitor demonstrated good electrochemical performance, with an optimal specific capacitance of 94.6 F/g at 850°C. Additionally, it exhibited an optimal energy density of 12.8 Wh/kg and a power density of 245.516 W/kg. These results suggest that porous carbon derived from ANW biomass holds promise as a sustainable working electrode for green-supercapacitor.

Keywords: Activated carbon; areca-nut waste; biomass; electrode; supercapacitor

Received 06-09-2024 | Revised 13-10-2024 | Accepted 31-10-2024 | Published 30-11-2024

INTRODUCTION

The growth of the human population and the development of the global economy have led to an increasing demand for energy worldwide. It is estimated that by 2026, the demand for energy will double. Therefore, it is important to study the development of new and sustainable energy sources. Supercapacitors have attracted attention because they are a new type of energy storage device that has high power density, long service life, good cycle stability, and large capacity [1]. In addition, supercapacitors are efficient, green, and environmentally friendly energy storage devices [2]. However, the low energy density of supercapacitors is a weakness that limits their widespread application. To overcome these problems, the development of electrode materials is necessary because they are a key factor in improving the performance of high-performance supercapacitors [3].

Activated carbon is commonly used as an electrode material due to its affordability, stability, and good conductivity [4]. It's typically derived from coal, petroleum, and biomass. Biomass-derived activated carbon offers advantages such as abundant availability, unique porosity, sustainability, and environmental friendliness [5]. Previous studies have highlighted the exceptional properties of natural waste-based carbon materials, including their nano morphology, hierarchical pores, and hydrophilicity supporting heteroatom elements [6, 7]. For example, hierarchically porous carbon from biomass plane tree fruit fluffs achieved an energy density of 46.3 Wh/kg [8]. Porous carbon obtained from biomass garlic peels exhibited an energy density of 9.07 Wh/kg and a specific capacitance reaching 396.25 F/g [4]. Additionally, porous carbon from the jujube shell demonstrated a high

specific capacitance of 535 F/g with an energy density of 13.97 Wh/kg [9]. However, not all biomass can exhibit these characteristics through simple and environmentally friendly methods, requiring further intensive studies to identify potential biomass and environmentally friendly approaches. On the other hand, the areca-nut (AN) is a major horticultural crop in Indonesia, occupying 147,890 hectares and supplying 80% of the global AN demand [10]. The substantial area of AN plantations generates significant waste, including areca-nut waste (ANW), which contains 66.08% cellulose, 7.40% hemicellulose, 19.59% lignin, and other minor components [10, 11]. Given these contents, ANW holds promise as a raw material for activated carbon production.

Furthermore, one of the main ways to convert biomass into activated carbon is by using the thermochemical transformation method [12]. This method consists of two steps, namely carbonization and activation. Carbonization is the process of converting organic matter into carbon through low-temperature pyrolysis [13]. This process focuses on removing volatile compounds, and hydrocarbons and breaking down precursors until charred residue remains. Furthermore, the activation process involves the addition of appropriate activating agents to obtain a high surface area with its unique porosity. The activation process is divided into two, namely chemical activation and physical activation. The chemical activation process is a common method used to produce carbon-based activated carbon derived from biomass [14]. In this process, biomass carbon material is mixed with chemicals and carbonized using inert gas. While the physical activation process uses oxygen-containing gases such as CO_2 and water vapor. This process takes place at high temperatures (800°C – 1000°C) by decomposing carbon materials so that they form many pores and cracks [15].

In this study, a simple and cost-effective synthesis is reported to obtain biomass-based activated carbon. Conversion of ANW into carbon through drying, pre-carbonization, chemical activation, carbonization, and physical activation processes. Chemical activation was carried out using 1 M $ZnCl_2$ as an activating agent. Carbon samples were prepared in powder form which were then carbonized and physically activated. Carbonization was carried out up to a temperature of 600°C with an inert gas environment (N_2). Physical activation was applied using different temperatures, namely at 800°C, 850°C, and 900°C with a CO_2 gas environment. Furthermore, the electrochemical performance of the activated carbon obtained was evaluated in a 2-electrode configuration with a specific capacitance of 94.6 F/g with an energy density of 12.8 Wh/kg and a power density of 245.516 W/kg. Therefore, this study proves that ANW biomass can be utilized as activated carbon to be used as an electrode supercapacitor.

MATERIALS AND METHODS

Material

Samples of ANW were collected from plantations in Solok Regency, Indonesia. We used $ZnCl_2$ from Merck KgA as the chemical activator. The gases N_2 and CO_2 were obtained from PT. Aneka Gas Industri Tbk, Indonesia. The electrolyte material H_2SO_4 was supplied by Panreac Química Sau. Duck eggshell membranes were used as separators, and DI water was produced on the laboratory scale.

Preparation of Sample Powder

The ANW was initially cleaned and cut into small pieces measuring 3 × 2 cm. Afterward, it was dried using sunlight for 2 days and then in an oven at 110°C for 48 hours. The drying process was then continued using a vacuum oven at a temperature range of 50°C – 250°C. Subsequently, the sample was ground using a mortar and ball milling. After grinding, the sample was sieved to obtain a uniform powder size of < 60 μm.

Preparation of Porous Carbon from ANW

The ANW sample powder was chemically impregnated using 1 M $ZnCl_2$ with distilled water and carbon. This process involved using a hotplate set to a rotation of 300 rpm and a temperature of 80°C. After impregnation, the sample was dried in an oven and then ground into powder again. The obtained carbon powder was subjected to pyrolysis through carbonization and physical activation. Carbonization was carried out at temperatures ranging from 30°C to 289°C and from 289°C to 600°C, with a N_2 gas flow rate of 1°C/min and 3°C/min, respectively. Physical activation was performed using CO_2 gas at temperatures of 800°C, 850°C, and 900°C, with a gas flow rate of 10°C/min. The resulting porous carbons were labeled as ANW-800, ANW-850, and ANW-900. The pyrolysis products were neutralized using DI water until the pH reached 7 and then dried in an oven at 110°C.

Material Characterization

Phase and degree of crystallinity of ANW were evaluated using X-ray diffraction (XRD) with a Shimadzu type MAXima_X, within the angle range (2θ) 10° – 60°, with plate number 1 No. BMN: 3.08.02.01.027.1. The electrochemical properties of the supercapacitor cell were evaluated in a two-electrode system using additional adhesive. The electrodes, with a diameter of 8 mm and a thickness of 0.2 mm, were prepared in a 1 M H_2SO_4 electrolyte solution and separated using a duck eggshell membrane. The electrochemical performance was measured using cyclic voltammetry (CV) and galvanostatic charge discharge (GCD) techniques. The CV method was carried out using a CV UR Rad-ER 5841 physics instrument, testing at a maximum voltage window of up to 1 V at scan rates of 1, 2, 5, and 10 mV/s. The GCD method was carried out using a CD UR Red-ER 2018 with a current density of 1 A/g. Specific capacitance, resistance, energy density, and power density were obtained from the CV and GCD methods, and calculated using standard equations.

RESULTS AND DISCUSSION

The XRD pattern of ANW at different physical activation temperatures is characterized in Figure 1. This pattern shows two diffraction peaks at 2θ values of 22.424° – 23.496° and 42.013° – 44.714° which are related to the crystal planes (002) and (100). This characteristic indicates low graphitization so that the activated carbon electrode has an amorphous nature [16]. Therefore, this structure can form more developed pores which results in high electrical conductivity values. High conductivity values can support better electrochemical properties. This study is in line with previous studies using different biomass, namely *Mangifera indica* leaf [17], *Phyllostachys edulis* [18], and paddy straw [19]. Furthermore, the XRD pattern also shows several sharp peaks which confirm the presence of crystalline compounds in each sample.

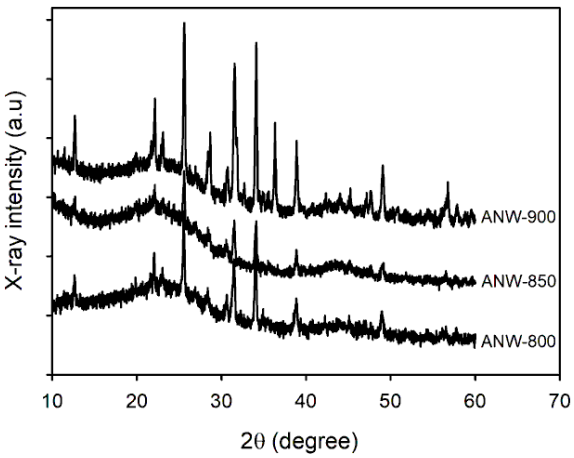

Figure 1. XRD pattern of ANW samples.

Table 1 shows the interlayer d-spacing and microcrystalline dimensions for the three ANW samples. The d_{002} and d_{100} values of ANW based on the Bragg equation $2d\sin\theta = n\lambda$ have values ranging from 3.783 – 3.962 Å and 2.025 – 2.148 Å, respectively. The d_{002} value obtained is higher than the d_{002} value of graphite confirming that the ANW-activated carbon sample has high porosity due to weak graphitization so that the sample has better

amorphous properties. Furthermore, the layer height value (L_c) is related to the specific surface area according to the empirical formula ($SSA_{xrd} = 2/\rho_{xrd}L_c$), where $\rho_{xrd} = (d_{002(graphite)}/d_{002}) \times \rho_{graphite}$ [20]. Based on the empirical formula, it can be concluded that the L_c value is inversely proportional to the specific surface area value. If the L_c value is small, the surface area is large. From Table 1, it can be seen that ANW-850 has the smallest Lc layer height value, which is 8.606 Å, so ANW-850 has the highest specific surface area which can improve the performance of supercapacitor electrodes.

Table 1. Lattice parameters and interlayer spacing for ANW activated carbon samples.

Samples code	$2\theta_{002}$ (°)	$2\theta_{001}$ (°)	d_{002} (Å)	d_{100} (Å)	L_c (Å)	L_a (Å)
ANW-800	22.424	44.714	3.962	2.025	8.982	15.619
ANW-850	23.496	44.128	3.783	2.050	8.606	36.752
ANW-900	22.913	42.013	3.878	2.148	9.177	10.505

The electrochemical properties of ANW were evaluated through a two-electrode system in 1 M H_2SO_4 electrolyte using CV and GCD. Figure 2 depicts the CV curves for the three electrodes at a scan rate of 1 mV/s with a voltage range of 0 – 1 V. The curves have a distorted rectangular shape, indicating the characteristics of the electrical double-layer capacitance derived from the porous carbon material [21]. The sample ANW-800 shows a fairly large hysteresis curve, which indicates a specific capacitance value of 60 F/g. Increasing the physical activation temperature significantly increases the current density of ANW-850, with its specific capacitance reaching 76 F/g. However, further increasing the physical activation temperature to 900°C reduces the current density in the hysteresis loop, confirming that the specific capacitive property of the third electrode decreases to 14 F/g.

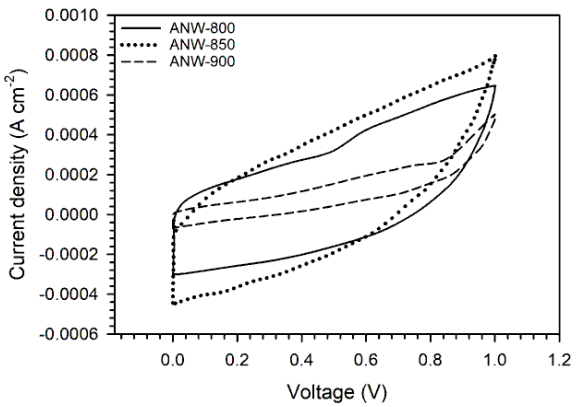

Figure 2. CV profile of ANW sample at a scan rate of 1 mV/s.

Furthermore, the electrode potential of ANW-850 was evaluated at different scan rates ranging from 1 to 10 mV/s, as shown in Figure 3. The figure illustrates that at high scan rates, the ANW-850 sample displays a good rectangular curve, which indicates ideal capacitive behavior characteristics [22]. However, at higher scan rates, the ions have enough time to diffuse into the electrode pores, the electrolyte ions are unable to access the interior of the active material, leading to a decrease in capacitance [23, 24].

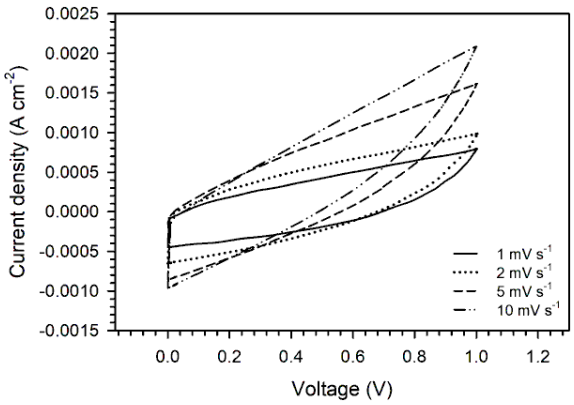

Figure 3. The CV profiles of ANW-850 at scan rates of 1, 2, and 5 mV/s.

The electrochemical performance of ANW-850 was thoroughly analyzed through GCD measurements. The GCD curve of ANW-850 was assessed at a current density of 1 A/g, as depicted in Figure 4. The results showed an isosceles triangle shape, confirming the normal double-layer electrochemistry [25]. In addition, the straight line on the discharge curve

indicated the ohmic resistance of the electrode [26]. The resistance value for ANW-850 was determined to be 0.27 Ω, with a specific capacitance of 94.6 F/g. Furthermore, the charge and discharge times on the GCD curve validated the coulombic efficiency value of the ANW-850 sample, which was found to be 87% [27]. These findings confirmed the superior electrochemical performance of the ANW-850 sample. In particular, the electrochemical performance of ANW-850 showed a specific capacitance of 94.6 F/g, accompanied by an energy density of 12.8 Wh/kg and a power density of 245.516 W/kg. The electrochemical performance of ANW was compared with that of other biomass-based activated carbon supercapacitor electrodes, as shown in Table 2.

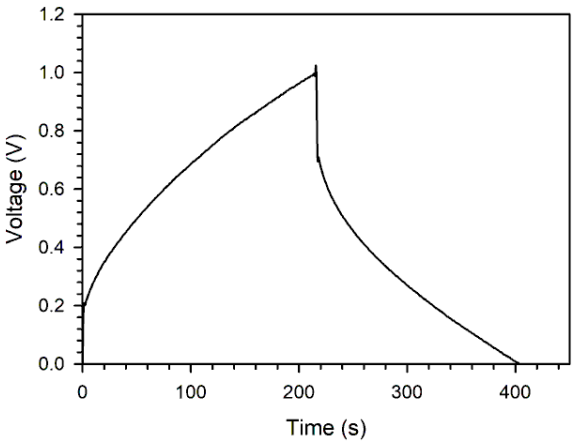

Figure 4. The GCD profiles of ANW samples.

Tabel 2. Comparison of the electrochemical performance of activated carbon-based supercapacitor electrodes derived from biomass.

sources	Csp (F/g)	Esp (Wh/kg)	Psp (W/kg)	References
Jack wood tree	147	8.02	68.5	[28]
Asparagus waste	160	31	560	[29]
Cashew nut shells	106	2.43	1002	[30]
Palm waste	135.1	3.4	202.6	[31]
Areca-nut waste	94.6	12.8	245.51	In this study

CONCLUSION

Porous carbon based on areca nut waste biomass has been successfully obtained through a simple method. The method begins with drying, pre-carbonization, chemical activation using 1 M $ZnCl_2$, and high-temperature pyrolysis (carbonization and physical activation). Physical activation was carried out with different temperature treatments, namely 800°C, 850°C, and 900°C. The activated carbon obtained has an amorphous structure with a 2θ angle of 22.424° – 23.496° and 42.013° – 44.714°. ANW-850 has the smallest L_c value of 8.606 Å, indicating a larger surface area than the other two samples. The electrochemical performance of ANW was also evaluated through a CV with specific capacitances of 60, 76, and 14 F/g for ANW-800, ANW-850, and ANW-900, respectively. Further electrochemical performance of ANW-850 was also evaluated using GCD which obtained a specific capacitance of 94.6 F/g with an energy density of 12.8 Wh/kg and a power density of 245.516 W/kg at a current density of 1 A/g. Thus, it can be concluded that the areca nut waste is suitable to be used as a carbon source for application in high-performance supercapacitor electrodes.

ACKNOWLEDGMENTS

The research was funded by Direktorat Jenderal Pendidikan Tinggi, Riset dan Teknologi, Republic of Indonesia in master thesis research-postgraduate program scheme with contract number of 20728/UN19.5.1.3/AL.04/2024.

REFERENCES

1. Wang, W., Shen, Y., Ma, Z., Wei, X., Fan, H., & Bai, Q. (2024). High-performance supercapacitors based on self-supporting thick carbon electrodes from renewable

biomass wood. *Sustainable Materials and Technologies*, **40**, e00824.
2. Hu, H., Yan, M., Jiang, J., Huang, A., Cai, S., Lan, L., Ye, K., Chen, D., Tang, K., Zuo, Q., Zeng, Y., & Zhao, Y. (2023). A state-of-the-art review on biomass-derived carbon materials for supercapacitor applications: From precursor selection to design optimization. *Science of The Total Environment*, 169141.
3. Liu, L., Zhang, W., Lu, B., Cheng, Z., Cao, H., Li, J., Fan, Z., & An, X. (2024). Controllable heteroatoms doped electrodes engineered by biomass based carbon for advanced supercapacitors: A review. *Biomass and Bioenergy*, **186**, 107265.
4. Liu, S., Dong, K., Guo, F., Wang, J., Tang, B., Kong, L., Zhao, N., Hou, Y., Chang, J., & Li, H. (2024). Facile and green synthesis of biomass-derived N, O-doped hierarchical porous carbons for high-performance supercapacitor application. *Journal of Analytical and Applied Pyrolysis*, **177**, 106278.
5. Yuksel, R. & Karakehya, N. (2024). High energy density biomass-derived activated carbon materials for sustainable energy storage. *Carbon*, **221**, 118934.
6. Taer, E., Yanti, N., Apriwandi, A., Ismardi, A., & Taslim, R. (2023). Novel O, P, S self-doped with 3D hierarchy porous carbon from aromatic agricultural waste via H_3PO_4 activation for supercapacitor electrodes. *Diamond and Related Materials*, **140**, 110415.
7. Taer, E., Apriwandi, A., Farma, R., & Taslim, R. (2024). Synthesis of highly self-NO-dual doped unique carbon blooming flower-like nanofiber derived novel snake-plant waste for ultrahigh energy of solid-state-supercapacitor. *Chemical Engineering Science*, **285**, 119566.
8. Wang, M. X., He, D., Zhu, M., Wu, L., Wang, Z., Huang, Z. H., & Yang, H. (2023). Green fabrication of hierarchically porous carbon microtubes from biomass waste via self-activation for high-energy-density supercapacitor. *Journal of Power Sources*, **560**, 232703.
9. Li, Y. & Qi, B. (2023). Secondary utilization of jujube shell bio-waste into biomass carbon for supercapacitor electrode materials study. *Electrochemistry Communications*, **152**, 107512.
10. Ridho, M. R., Nawawi, D. S., Juliana, I., & Fatriasari, W. (2023). The kraft lignin characteristics of areca leaf sheath isolated by phosphoric acid. *Bioresource Technology Reports*, **23**, 101569.
11. Madyaratri, E. W., Ridho, M. R., Iswanto, A. H., Osvaldová, L. M., Lee, S. H., Antov, P., & Fatriasari, W. (2023). Effect of lignin or lignosulfonate addition on the fire resistance of areca (*Areca catechu*) particleboards bonded with ultra-low-emitting urea-formaldehyde resin. *Fire*, **6**(8), 299.
12. Tekin, B. & Topcu, Y. (2024). Novel hemp biomass-derived activated carbon as cathode material for aqueous zinc-ion hybrid supercapacitors: Synthesis, characterization, and electrochemical performance. *Journal of Energy Storage*, **77**, 109879.
13. Muttil, N., Jagadeesan, S., Chanda, A., Duke, M., & Singh, S. K. (2022). Production, types, and applications of activated carbon derived from waste tyres: an overview. *Applied Sciences*, **13**(1), 257.
14. Taer, E., & Taslim, R. (2020). A high potential of biomass leaves waste for porous activated carbon nanofiber/nanosheet as electrode material of supercapacitor. *Journal of Physics: Conference Series*, **1655**(1), 012007.
15. Qiu, C., Jiang, L., Gao, Y., & Sheng, L. (2023). Effects of oxygen-containing functional groups on carbon materials in supercapacitors: A review. *Materials and Design*, **230**, 111952.
16. Ma, Y., Tian, J., Li, L., Kong, L., Liu, S., Guo, K., & Chen, X. (2021). Interconnected hierarchical porous carbon synthesized from freeze-dried celery for supercapacitor with high performance.

International Journal of Energy Research, **45**(6), 9058–9068.
17. Hegde, S. S. & Bhat, B. R. (2024). Sustainable energy storage: Mangifera indica leaf waste-derived activated carbon for long-life, high-performance supercapacitors. *RSC advances*, **14**(12), 8028–8038.
18. Egun, I. L., Akinwolemiwa, B., Yin, B., Tian, H., He, H., Fow, K. L., Zhang, H., Chen, G. Z., & Hu, D. (2024). Conversion of high moisture biomass to hierarchical porous carbon via molten base carbonisation and activation for electrochemical double layer capacitor. *Bioresource Technology*, **409**, 131251.
19. Devi, R., Kumar, V., Kumar, S., Bulla, M., & Mishra, A. K. (2024). Performance optimization of the symmetric supercapacitors based on paddy straw-derived porous activated carbon. *Journal of Energy Storage*, **79**, 110167.
20. Kumar, K., Saxena, R. K., Kothari, R., Suri, D. K., Kaushik, N. K., & Bohra, J. N. (1997). Correlation between adsorption and X-ray diffraction studies on viscose rayon based activated carbon cloth. *Carbon*, **35**(12), 1842–1844.
21. Tadesse, M. G., Kasaw, E., & Lübben, J. F. (2023). Valorization of banana peel using carbonization: Potential use in the sustainable manufacturing of flexible supercapacitors. *Micromachines*, **14**(2), 330.
22. Li, W., Chen, C., Wang, H., Li, P., Jiang, X., Yang, J., & Liu, J. (2022). Hierarchical porous carbon induced by inherent structure of eggplant as sustainable electrode material for high performance supercapacitor. *Journal of Materials Research and Technology*, **17**, 1540–1552.
23. Ozpinar, P., Dogan, C., Demiral, H., Morali, U., Erol, S., Samdan, C., Yildiz, D., & Demiral, I. (2022). Activated carbons prepared from hazelnut shell waste by phosphoric acid activation for supercapacitor electrode applications and comprehensive electrochemical analysis. *Renewable Energy*, **189**, 535–548.
24. Taer, E., Deraman, M., Taslim, R., & Iwantono. (2013). Preparation of binderless activated carbon monolith from pre-carbonization rubber wood sawdust by controlling of carbonization and activation condition. *AIP Conference Proceedings*, **1554**(1), 33–37.
25. Yue, W., Yu, Z., Zhang, X., Liu, H., Zhang, Y., & Ma, X. (2024). Preparation of natural N/O/S co-doped biomass-derived carbon materials for supercapacitors using multistage gas self-exfoliation effect. *Journal of Analytical and Applied Pyrolysis*, **179**, 106525.
26. Rahim, A. H. A., Ramli, N., Nordin, A. N., & Wahab, M. F. A. (2021). Supercapacitor performance with activated carbon and graphene nanoplatelets composite electrodes, and insights from the equivalent circuit model. *Carbon Trends*, **5**, 100101.
27. Joseph, S., Singh, G., Lee, J. M., Yu, X., Breese, M. B., Ruban, S. M., Bhargava, S. K., Yi, J., & Vinu, A. (2023). Hierarchical carbon structures from soft drink for multi-functional energy applications of Li-ion battery, Na-ion battery and CO_2 capture. *Carbon*, **210**, 118085.
28. Bandara, T. M. W. J., Alahakoon, A. M. B. S., Mellander, B. E., & Albinsson, I. (2024). Activated carbon synthesized from Jack wood biochar for high performing biomass derived composite double layer supercapacitors. *Carbon Trends*, **15**, 100359.
29. Ahmad, N., Rinaldi, A., Sidoli, M., Magnani, G., Morenghi, A., Scaravonati, S., Vezzoni, V., Pasetti, L., Fornasini, L., Ridi, F., Milanese, C., & Pontiroli, D. (2024). High performance quasi-solid-state supercapacitor based on activated carbon derived from asparagus waste. *Journal of Energy Storage*, **99**, 113267.

30. Chaiammart, N., Vignesh, V., Thu, M. M., Eiad-ua, A., Maiyalagan, T., & Panomsuwan, G. (2024). Chemically activated carbons derived from cashew nut shells as potential electrode materials for electrochemical supercapacitors. *Carbon Resources Conversion*, 100267.

31. Rustamaji, H., Prakoso, T., Devianto, H., Widiatmoko, P., Febriyanto, P., & Eviani, M. (2024). Modification of hydrochar derived from palm waste with thiourea to produce N, S co-doped activated carbon for supercapacitor. *Sustainable Chemistry for the Environment*, **7**, 100132.